5-2023

A Systematic Study into the Design and Utilization of Burn Wire as a means of Tensioning and Releasing Spacecraft Mechanisms through Applied Joule Heating

Chandler Dye
University of Arkansas, Fayetteville

A SYSTEMATIC STUDY INTO THE DESIGN AND UTILIZATION OF BURN WIRE AS A MEANS OF TENSIONING AND RELEASING SPACECRAFT MECHANISMS THROUGH APPLIED JOULE HEATING

Undergraduate Honors Thesis

Chandler Dye

May 2023

Submitted to the Faculty of the University of Arkansas

In Partial Fulfillment of the Requirements for the degree of

Bachelor of Science in Mechanical Engineering

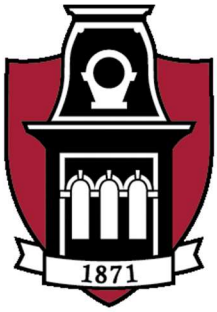

UNIVERSITY OF ARKANSAS

College of Engineering
Mechanical Engineering

Department of Mechanical Engineering

Fayetteville, Arkansas

ABSTRACT

The joule heating characteristics of Nichrome burn wires, often used as a thermal cutting device in mechanisms designed to fasten and release CubeSat deployables, are examined in the following thesis. Wires ranging from 0.125 inches to 2 inches long, and diameters of 30 Ga and 40 Ga, are investigated through analytical calculations and thermal simulations based on heat transfer due to joule heating, and through physical circuitry-based experiments. The temperature data is used to generate heating curves to predict the time it takes for Nichrome wires to fail under varying testing parameters. This research aims to catalog a series of data for future use relating to the heating characteristics of Nichrome wires for spacecraft applications. It also serves as a starting point for future research into utilizing the wire as a stand-alone mechanism for fastening and deploying spacecraft deployables as opposed to the NRL burn wire mechanism that is the standard. This research will be used to inspire further research into alternatives to the NRL design that will benefit the CubeSat program at the University of Arkansas.

TABLE OF CONTENTS

1. ACKNOWLEDGEMENTS

I would like to thank the University of Arkansas and the University of Arkansas Department of Mechanical Engineering for their support throughout the Honors program process. I would also like to thank Dr. Adam Huang for giving me the opportunity to pursue this research and for his continued support as an advisor. I would also like to thank the various members of Dr. Adam Huang's research team, namely Cass Wiederkehr, Ethan Graef, Samuel Cano, Charles Smith, and Mattie Mclellan, for their encouragement and helpful feedback at each weekly progress update meeting. It has been wonderful hearing about your research developments and getting to know you all.

2. NOMENCLATURE

A_{cs}	cross-sectional area (m^2)
A_s	surface area exposed to the ambient environment (m^2)
K_s	thermal conduction coefficient (W/m/K)
T_0	ambient temperature and the initial temperature of the wire (K)
ρ_r	resistivity of the wire (Ω*m)
℃	degrees Celsius
h	convective heat transfer coefficient ($W/m^2/K$)
Ga	wire gauge, determines wire diameter
I	applied current (A)
K	degrees Kelvin
P	power (Watts)
R	resistance of the wire (Ω)
T	temperature of the wire (K)
V	volume of the wire (m^3)
c	specific heat (J/kg/K)
kg	kilogram
l	wire length (m)
t	time (s)
ε	emissivity
ρ	density of the wire (kg/m^3)
σ	Stefan-Boltzmann constant, equal to 5.6704E-8 ($W/m^2/K$)
∂	partial derivative
NRL	Naval Research Laboratory

3. INTRODUCTION

3.1 Background

The development of satellites began during the Cold War as a competition between nations to push the envelope and reach milestones in scientific advancements before the other, but satellites have evolved to play a critical role in humanities understanding of the origins and development of the universe. With the increased interest in advancing satellite technology to make designing and building them more accessible and cost-effective, there have been numerous iterations on alternatives to the traditional satellite model to make satellite development something that anyone can do, not just national space entities. One of these alternatives is the CubeSat model, a cubic-shaped miniature satellite with dimensions of 10 cm^3 which is typically designed and used by engineers, scientists, and students for technology demonstrations or simple experimental applications in a space environment (typically in low-earth orbit). Roughly the size of a Rubik's cube, they weigh about 1 kg and can be used alone (1 unit) or grouped and stacked together in multiple units depending on the complication of the mission (with a max of 24 units) [1]. Developed by professors Jordi Puig-Suari of Cal Poly and Bob Twiggs of Stanford in 1999, the original intention behind the creation of the CubeSat design was to give graduate students the ability to design, build, test, and operate the limited capabilities of an artificial satellite within the limited time and financial constraints of a graduate degree program [2]. Satellites are typically very expensive to build and launch, and because of this, they have historically been used for low-risk long-duration missions. This has naturally limited the participation and knowledge-gaining opportunities in the world of satellite development away from individuals and instead towards systems-level experts inside the satellite industry whose contributions to their subsystems are necessary to achieve precedent changing missions. While the invention of CubeSats has

benefitted students, they have also grown to be a staple in the industry due to their basic design and quick turnaround in terms of getting results. A whole new world of low-cost high-risk exploratory research missions are now available to researchers because of the inexpensive and quick development time of CubeSats [3]. Due to the high levels of interest in CubeSats in the space industry, it has become imperative that researchers investigate more ways to improve their design and utilization.

CubeSats traditionally use burn wire mechanisms for the restraint and deployment of deployable structures. The most widely used burn wire mechanism is the one invented by Adam Thurn, an Aerospace Engineer at the U.S. Naval Research Laboratory (NRL) [4]. The burn wire in the NRL mechanism is made from nickel chromium, or Nichrome, which is often used in heating elements because of its high electrical resistance. In their setup, a current is run through the burn wire so that the wire acts as a resistor and rapidly heats up due to joule heating. Once it has reached a high enough temperature, it is then capable of thermally cutting through the tie down cable that it is in contact with so that a deployable structure on the spacecraft is released from its stowed configuration and is able to actuate into its flight configuration once the spacecraft reaches its operational orbit. The superiority of the NRL mechanism compared to other burn wire mechanisms stems from its low-cost and simplistic design which makes it conducive for researchers and university students alike to easily replicate and use for their own studies [4]. The problem with this design is the need for redundancy. Sometimes the tie down cable can come loose during vibration tests or launch ascent due to their low strength, and so two or more burn wires are often used to reduce the likelihood of the premature loosening of deployables [5]. This doubles the cost of what was initially a low-cost setup. To my knowledge

there has yet to be any further research into trying to improve this technology to a point where redundancy becomes unnecessary.

A goal of this research is to test the heat transfer characteristics of a Nichrome wire to see what possibilities exist for creating a burn wire mechanism that uses only one Nichrome burn wire as a means of fastening down and releasing deployable structures on CubeSats. In this paper, I investigate the transient heat transfer process of a Nichrome burn wire due to joule heating at various wire lengths, wire gauges, and various constant applied power values in terms of Watts/inch, with the goal of determining the time it takes for the wire to fail, or separate, at these varied parameters. The ultimate goal of this research is to document and tabulate these test results so that they can be used in future experiments. Due to time constraints, the wire is not tested at varied tension forces, though this would affect the failure time.

3.2 Objectives

The objectives of this paper and the experiment outlined herein are as follows:

- To investigate the heating characteristics of a Nichrome wire (lengths ranging from 0.125in to 2in and gauges varying from 40 Ga to 30 Ga) under a constant power model using different means of calculation (analytical calculation, SolidWorks simulation, COMSOL simulation, physical experiments).
- Tabulate this data for future internal use and develop a skillset that can be used to continue this work for my master's research.

3.3 Theory

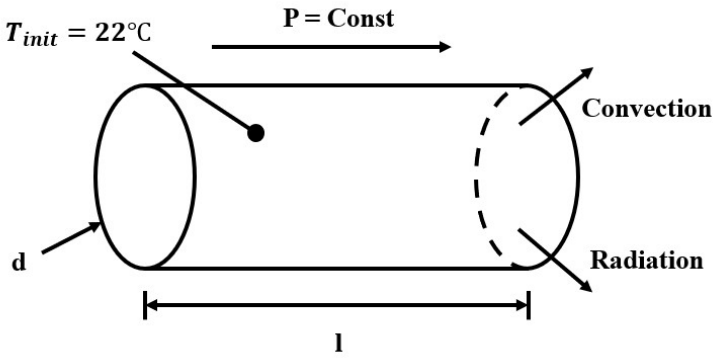

Figure 3.1 - Constant Power Heat Transfer Model Diagram.

The joule heating of a Nichrome burn wire can be treated as a generally simple heat transfer problem. The general form of the heat transfer equation is,

$$\underbrace{A_{cs}\frac{\partial}{\partial x}\left(K_s\frac{\partial T}{\partial x}\right)l}_{Conduction} + \underbrace{\frac{I^2\rho_r l}{A_{cs}}}_{Heat\ Gen.\ Rate} - \underbrace{hA_s(T-T_0)}_{Convection} - \underbrace{\sigma\varepsilon A_s\left(T^4-{T_0}^4\right)}_{Radiation} = \underbrace{c\rho V\frac{\partial T}{\partial t}}_{Heat\ Storage} \qquad \text{(E1)}$$

where A_{cs} is the cross-sectional area (m^2), equal to πr^2, K_s is the thermal conduction coefficient (W/m/K), T is the temperature of the wire (K), l is the wire length (m), I is the applied current (A), ρ_r is the resistivity of the wire (Ω*m), h is the convective heat transfer coefficient ($W/m^2/K$), A_s is the surface area exposed to the ambient environment (m^2), T_0 is the ambient temperature and the initial temperature of the wire (K), σ is the Stefan-Boltzmann constant, equal to 5.6704E-8 ($W/m^2/K$), ε is the emissivity value, which we will assume is equal to 0.8, c is the specific heat (J/kg/K), ρ is the density of the wire (kg/m^3), V is the volume of the wire (m^3), equal to $A_{cs} * l$, and t is time (s). Assuming that the joule heating is uniform across the wire, and that there is relatively no temperature gradient across the length of the wire, the

conduction term can be eliminated. Realistically, ρ_r changes as temperature increases, but we can use a constant power model in which I makes up for this change, and $\frac{I^2\rho_r l}{A}$, which is equal to P, will be a constant in our equation. After replacing $\frac{I^2\rho_r l}{A}$ with P, and $\frac{\partial T}{\partial t}$ with $\frac{T_n - T_{n-1}}{dt}$, and rearranging the equation, we are left with:

$$P - hA_s(T - T_0) - \sigma\varepsilon A_s\left(T^4 - {T_0}^4\right) = c\rho V\frac{T_n - T_{n-1}}{dt} \quad \text{(E2)}$$

If we rearrange the equation once more, solving for T_n, we are left with:

$$\frac{P - hA_s(T - T_0) - \sigma\varepsilon\ _s\left(T^4 - {T_0}^4\right)}{c\rho V}dt + T_{n-1} = T_n \quad \text{(E3)}$$

This equation allows for the calculation of the wire temperature at certain time steps, n, using the previous wire temperature and the gained thermal energy after a certain amount of time, dt. Another way to look at this heat transfer problem is to focus on the energy balance. Using this perspective, it is easier to separate the various parameters that affect the wire temperature over time. In equation E4, E_{stored} increases over time as energy builds up in the system and increases the temperature of the wire.

$$E_{stored} = c * \rho * V * (T_n - T_0) \quad \text{(E4)}$$

The energy balance can be treated as "Gain of thermal energy = Heating Flux - Cooling Flux." This is shown in equation E5 in which the net energy is equal to the energy in minus the energy out.

$$E_{net} = E_{in} - E_{out} = c * \rho * V * (T_n - T_{n-1}) \quad \text{(E5)}$$

Energy in comes from the joule heating of the wire. The value dt is determined from the step size chosen between energy balance calculations.

$$E_{in} = P * dt \tag{E6}$$

Energy out in air comes from two sources: convection, and radiation out from the surface of the wire.

$$E_{out(convection)} = h * A_s * (T_{n-1} - T_0) * dt \tag{E7}$$

$$E_{out(radiation)} = \sigma * \varepsilon * A_s * [(T_{n-1})^4 - (T_0)^4] * dt \tag{E8}$$

Combining these in equation E5, and solving for T_n, we are left with equation E9:

$$T_n = T_{n-1} + \frac{P*dt - h*A_s*(T_{n-1}-T_0)*dt - \sigma*\varepsilon*A_s*[(T_{n-1})^4-(T_0)^4]*dt}{c*\rho*V} \tag{E9}$$

Equation E9 uses the initial conditions, $E_{out} = 0$ @ $t = 0$, and $E_{in} \neq 0$ @ $t = 0$ to properly set up the Excel sheet for each testing scenario. The value for $I^2 * R$ is constant in a constant power application. In a vacuum environment, there is no E_{out} from convection, and there is very little E_{out} from radiation, so these values will be treated as equal to 0 in the vacuum calculations.

4. ANALYSIS & EXPERIMENTAL METHODS

4.1 Analytical Calculations

For the analytical calculations, Excel was used to make iterating through time steps an efficient process. Shown below are the constants that were used in each testing scenario.

Analytical Parameters in Air

Parameter	Value	Unit
T_0	22	°C
Power	P	W
dt	0.01	s
h_amb	25	W/(m^2*K)
Diam	d	m
A_cs	π*d^2/4	m^2
Length	l	m
A_s	π*d*l	m^2
V	A_cs*l	m^3
ρ	8310	kg/m^3
Mass	ρ*V	kg
c	448	J/(kg*K)
k	15	W/(m*K)
ε	0.8	
σ	5.67037E-08	W/(m^2*K)

Analytical Parameters in Vacuum

Parameter	Value	Unit
T_0	22	°C
Power	P	W
dt	0.01	s
h_amb	0	W/(m^2*K)
Diam	d	m
A_cs	π*d^2/4	m^2
Length	l	m
A_s	π*d*l	m^2
V	A_cs*l	m^3
ρ	8310	kg/m^3
Mass	ρ*V	kg
c	448	J/(kg*K)
k	15	W/(m*K)
ε	0	
σ	5.67037E-08	W/(m^2*K)

Figure 4.1 – Analytical Calculation Parameters for Air and Vacuum in Excel.

Power in each test is a constant that is dependent on the length of the wire since it is in Watts/inch. Diameter is determined by the gauge of the wire we use as shown in Figure 4.2.

Gauge	Diam (in)	Diam (m)	Rad (in)	Rad (m)	A_cs (in^2)	A_cs (m^2)
40	0.003145	7.9883E-05	0.001573	3.99415E-05	7.76839E-06	5.01186E-09
39	0.003531	8.9687E-05	0.001766	4.48437E-05	9.79231E-06	6.31761E-09
38	0.003965	0.00010071	0.001983	5.03555E-05	1.23474E-05	7.96606E-09
37	0.004453	0.00011311	0.002227	5.65531E-05	1.55738E-05	1.00476E-08
36	0.005000	0.000127	0.002500	0.0000635	1.9635E-05	1.26677E-08
35	0.005615	0.00014262	0.002808	7.13105E-05	2.47622E-05	1.59756E-08
34	0.006305	0.00016015	0.003153	8.00735E-05	3.1222E-05	2.01432E-08
33	0.007080	0.00017983	0.003540	0.000089916	3.93692E-05	2.53994E-08
32	0.007950	0.00020193	0.003975	0.000100965	4.96391E-05	3.20252E-08
31	0.008928	0.00022677	0.004464	0.000113386	6.26034E-05	4.03892E-08
30	0.010025	0.00025464	0.005013	0.000127318	7.8933E-05	5.09244E-08

Figure 4.2 – Diameter, Radius, and Cross-Sectional Area Values for Different Wire Gauges.

Length will vary from test to test, ranging from 0.125 inches to 2 inches, to see what effect it has on the time to failure. Going from air to vacuum, the values for emissivity and the convective heat transfer coefficient will become zero to eliminate the terms for radiation and convection. Using equations E4-E9, in a constant 1 Watt/inch model, on a 40 Ga Nichrome wire, the temperature of the wire was calculated over time for both air and vacuum environments.

Analytical Iteration in Air

Time (s)	E_rad	E_conv	E_net	E_stored	T_wire
0	0	0	0.00125	0	22
0.01	0	0	0.00125	0.00125	43.1003
0.02	1.16E-09	4.20317E-06	0.001246	0.0025	64.2006
0.03	6.06E-09	8.40633E-06	0.001242	0.003746	85.22993
0.04	1.9E-08	1.25954E-05	0.001237	0.004987	106.1882
0.05	4.59E-08	1.67702E-05	0.001233	0.006225	127.0756
0.06	9.42E-08	2.0931E-05	0.001229	0.007458	147.892
0.07	1.73E-07	2.50776E-05	0.001225	0.008687	168.6374
0.08	2.92E-07	2.92101E-05	0.00122	0.009912	189.3115
0.09	4.64E-07	3.33283E-05	0.001216	0.011132	209.9138
0.1	7.02E-07	3.74323E-05	0.001212	0.012348	230.4437
0.11	1.02E-06	4.15218E-05	0.001207	0.01356	250.9002
0.12	1.43E-06	4.55968E-05	0.001203	0.014768	271.2824
0.13	1.96E-06	4.96569E-05	0.001198	0.015971	291.5889
0.14	2.61E-06	5.37019E-05	0.001194	0.017169	311.8179
0.15	3.42E-06	5.77315E-05	0.001189	0.018363	331.9676
0.16	4.39E-06	6.17454E-05	0.001184	0.019552	352.0357
0.17	5.55E-06	6.57429E-05	0.001179	0.020735	372.0196
0.18	6.92E-06	6.97237E-05	0.001173	0.021914	391.9165
0.19	8.53E-06	7.36871E-05	0.001168	0.023088	411.723
0.2	1.04E-05	7.76326E-05	0.001162	0.024255	431.4355
"	"	"	"	"	"

Analytical Iteration in Vacuum

Time (s)	E_rad	E_conv	E_net	E_stored	T_wire
0	0	0	0.00125	0	22
0.01	0	0	0.00125	0.00125	43.1003
0.02	0	0	0.00125	0.0025	64.2006
0.03	0	0	0.00125	0.00375	85.3009
0.04	0	0	0.00125	0.005	106.4012
0.05	0	0	0.00125	0.00625	127.5015
0.06	0	0	0.00125	0.0075	148.6018
0.07	0	0	0.00125	0.00875	169.7021
0.08	0	0	0.00125	0.01	190.8024
0.09	0	0	0.00125	0.01125	211.9027
0.1	0	0	0.00125	0.0125	233.003
0.11	0	0	0.00125	0.01375	254.1033
0.12	0	0	0.00125	0.015	275.2036
0.13	0	0	0.00125	0.01625	296.3039
0.14	0	0	0.00125	0.0175	317.4042
0.15	0	0	0.00125	0.01875	338.5045
0.16	0	0	0.00125	0.02	359.6048
0.17	0	0	0.00125	0.02125	380.7051
0.18	0	0	0.00125	0.0225	401.8054
0.19	0	0	0.00125	0.02375	422.9057
0.2	0	0	0.00125	0.025	444.006
"	"	"	"	"	"

Figure 4.3 – Excel Time Step Iteration in Air and Vacuum for l=0.125in.

Using this data, the wire temperature was graphed versus time. After changing the wire length and adjusting the Watts/inch accordingly, it was noted that these changes had no effect on the heating curves.

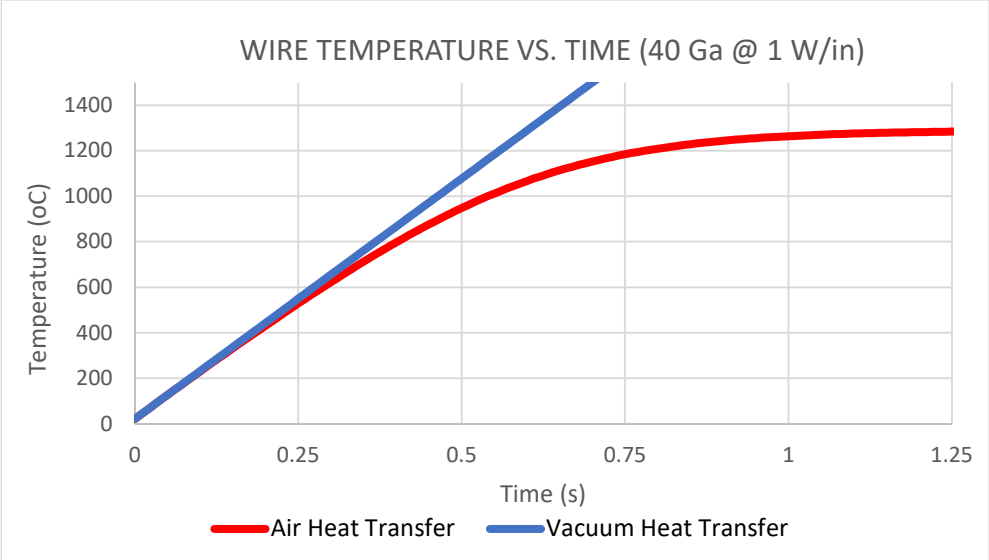

Figure 4.4 – 40 Ga Wire Temperature Curves in Air and in Vacuum for 1Watt/inch.

The vacuum thermal curve is linear and has a constant thermal energy increase over time, while the air thermal curve exhibits a logarithmic growth that settles at an equilibrium temperature. If the melting temperature of 1400°C is not met, assuming there are no outside forces acting on the wire, the wire will stay at the equilibrium temperature until more energy is added. If the melting temperature is reached, the wire will fail.

4.2 SolidWorks Simulations

The SolidWorks Simulation Thermal Analysis package covers heat transfer by conduction, convection and radiation, thermally induced stress, and thermally induced buckling [6]. For my purposes, I started with a steady-state simulation to gather initial temperature data from for the transient simulation. After applying material properties to a simple cylindrical SolidWorks part and inputting a volumetric temperature of 22°C, the steady-state analysis was run.

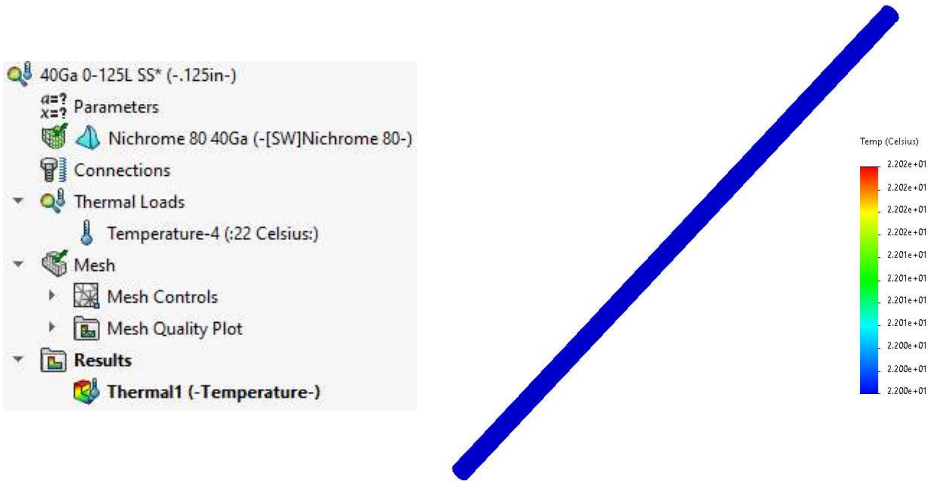

Figure 4.5 – SolidWorks Setup for Steady-State Thermal Simulation.

Using the data from the steady state as a base, this simulation was copied and turned into a transient simulation. A convection and radiation outward thermal load were applied to the model and could be disabled during vacuum simulations versus air simulations. A thermal sensor was input into the study at the center of the cylinder to measure the maximum temperature value across each time step.

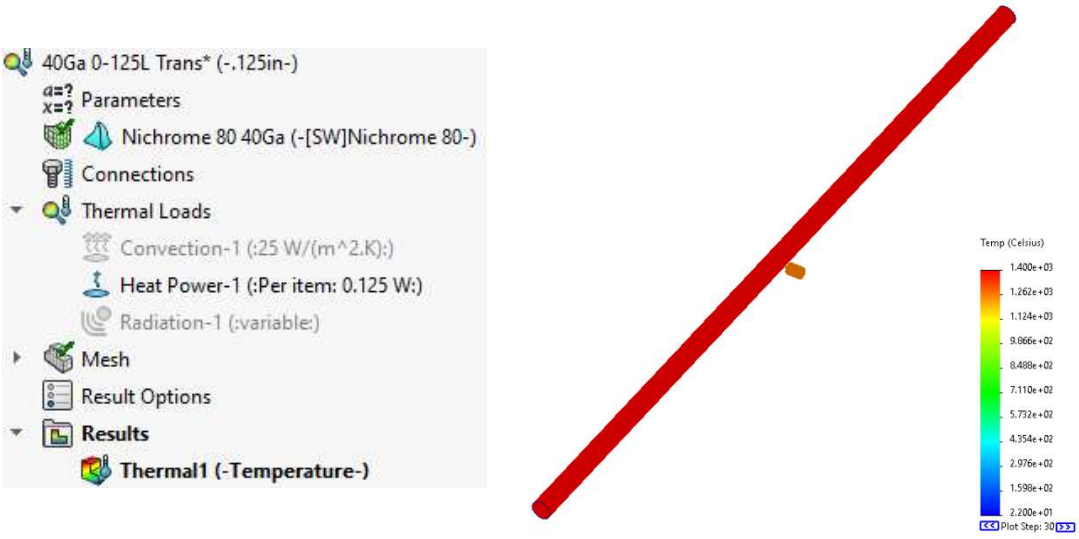

Figure 4.6 – SolidWorks Setup for Transient Thermal Simulation in Vacuum.

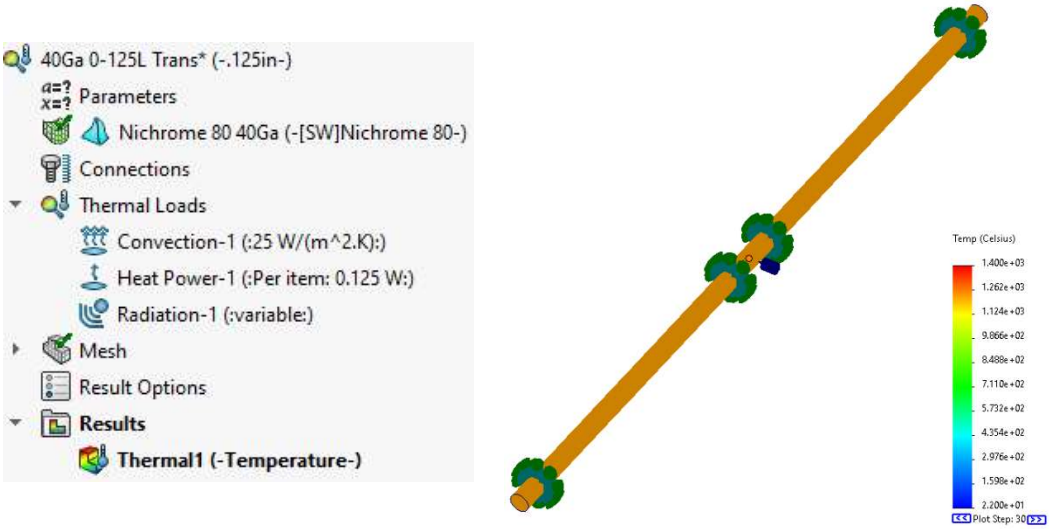

Figure 4.7 – SolidWorks Setup for Transient Thermal Simulation in Air.

Simulation data was exported to Excel and used to generate similar temperature curves to those in the analytical tests so that failure times can be calculated for these simulations.

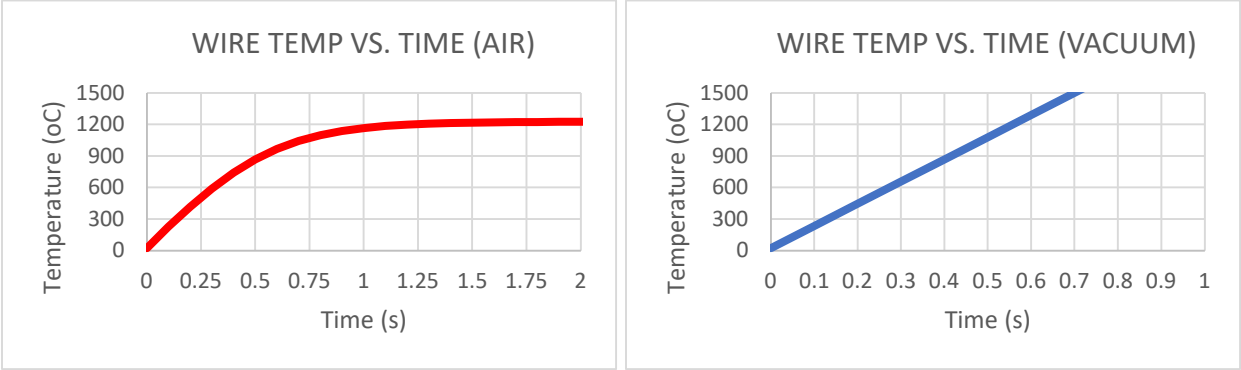

Figure 4.8 – SolidWorks Transient Temperature Graphs.

4.3 COMSOL Simulations

The Heat Transfer Module is an add-on to the COMSOL Multiphysics simulation platform. Like SolidWorks, COMSOL has the capability to simulate conduction, convection, and radiation heat transfer [7]. It also can combine multiple modules, such as the Heat Transfer

Module and the Electric Currents Module, to simulate complex multiphysics interactions, such as Joule Heating, more realistically [8]. After selecting the heat transfer physics package, and selecting the time dependent study option, a cylindrical model was created using the COMSOL model builder. The material library did not have the version of Nichrome I am conducting my physical tests on, so I had to create a custom material and manually input the material properties. The ambient temperature was set to 22°C, and the heat transfer modes were added. The heat source was applied to the whole volume of the cylinder, while the heat flux (convection) and diffuse surface (radiation) were applied to the external surface of the cylinder.

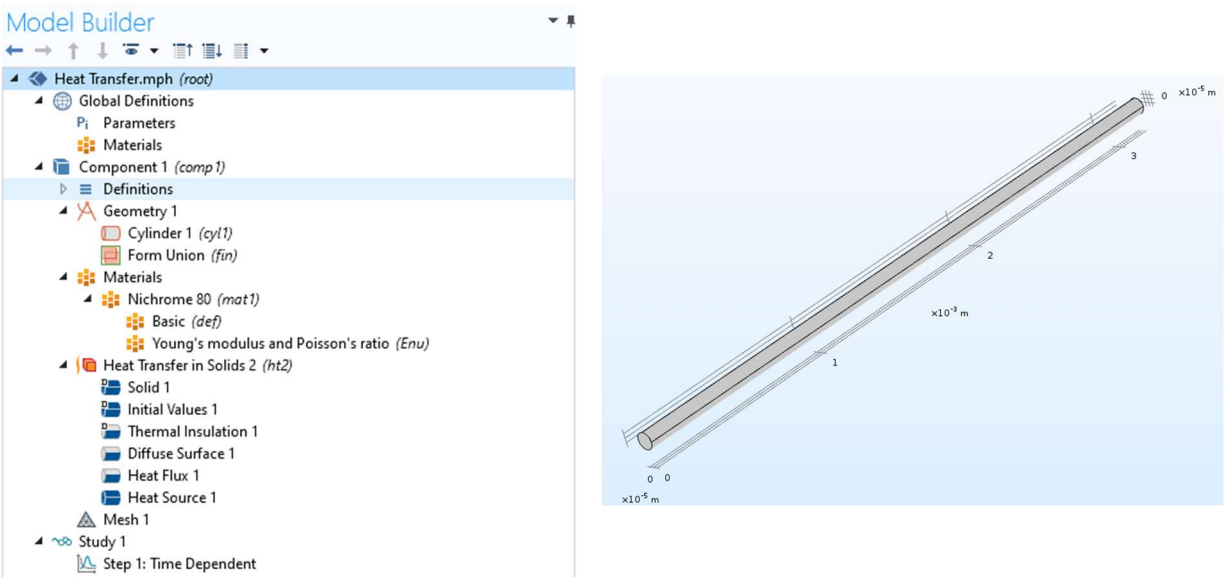

Figure 4.9 – COMSOL Model Builder Simulation Setup.

The study time for the time dependent study was adjusted for air simulations versus vacuum simulations due to their expected times to failure to cut down on computation time. A 3D cut point was added to the very center of the cylinder so that temperature data from this point could be exported to Excel.

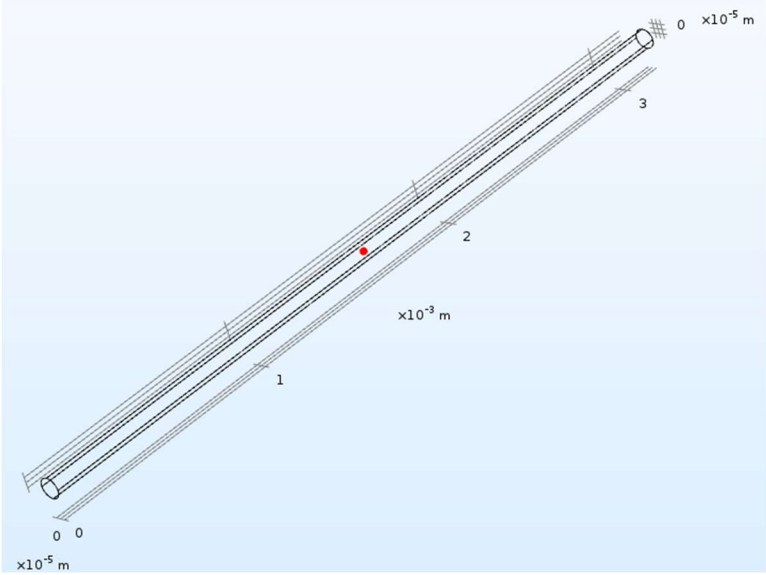

Figure 4.10 – COMSOL 3D Cut Point (in red).

The simulations were run for both the air and vacuum environments.

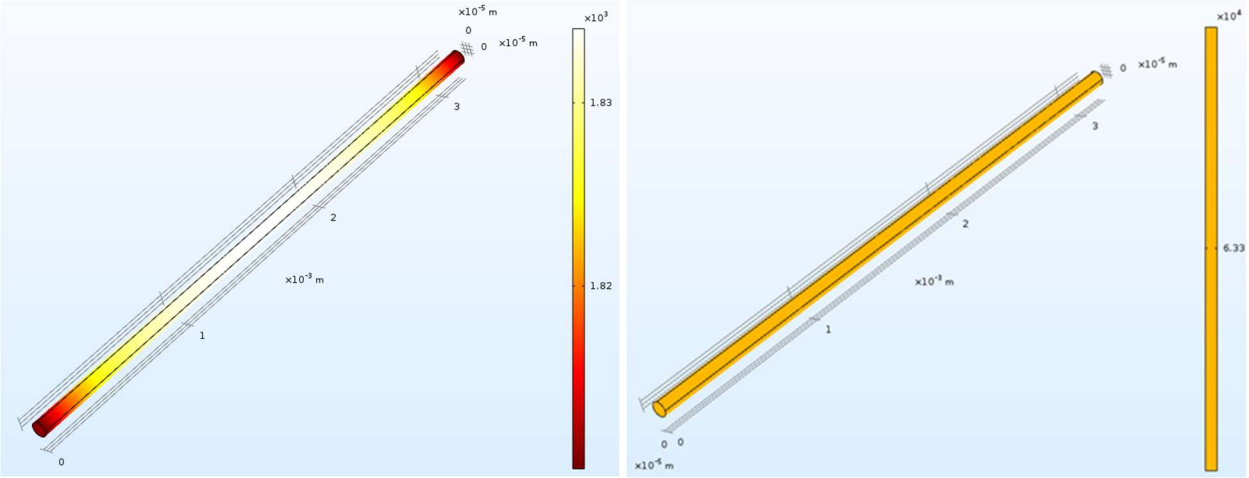

Figure 4.11 – COMSOL Transient Thermal Simulation in Air (left) and in Vacuum (right).

The data gathered from the 3D cut point was exported to Excel and used to generate similar graphs to the analytical and SolidWorks graphs that can be used to determine the failure time.

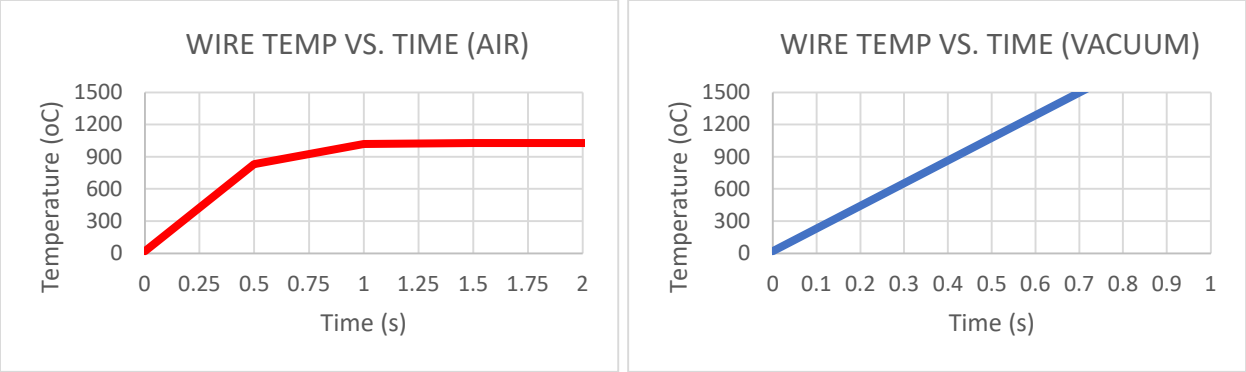

Figure 4.12 – COMSOL Transient Temperature Graphs.

4.4 Experimental Tests

For the physical experiments, I used a FLIR E60 thermal camera. This camera is designed to be used for electrical and mechanical inspections, but it can also be used for temperature-related experiments. Due to the odd shape of the camera, a mount had to be designed and 3D printed so that the camera could be mounted to a tripod.

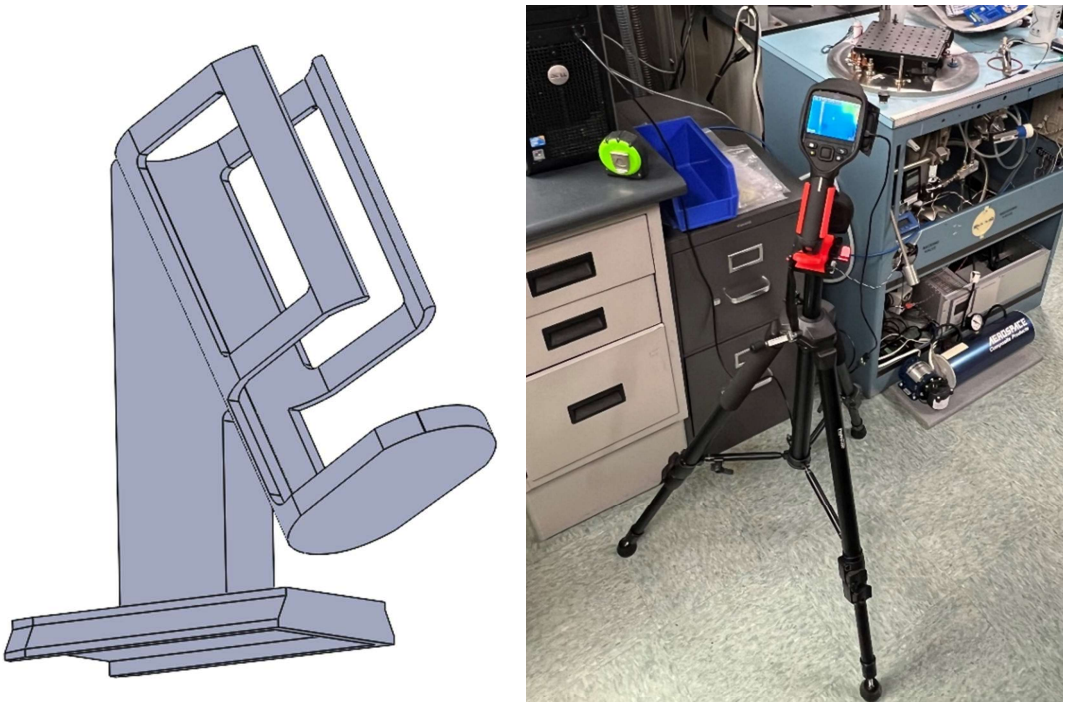

Figure 4.13 –Tripod Stand 3D CAD Model and FLIR E60 in Stand.

The FLIR E60 has two different object temperature ranges: -20°C to +120°C, and 0°C to +650°C. For these tests, the goal is to determine the temperature at failure and the time it takes for the wire to fail, under varying test conditions. Since there were no camera filters on hand that could detect object temperatures up to melting point, I went with the range of 0°C to +650°C and decided to make assumptions for the rest of the heating curve based on the time it took to fail. The camera was hooked to the computer using a USB cable and the FLIR ResearchIR software was used to track and record the temperatures of the wire over time. The wire mount was designed so that it worked with the prebuilt vacuum chamber base that was in the lab. Below is a picture of the 3D model for the testing mount and the actual testing mount in practice.

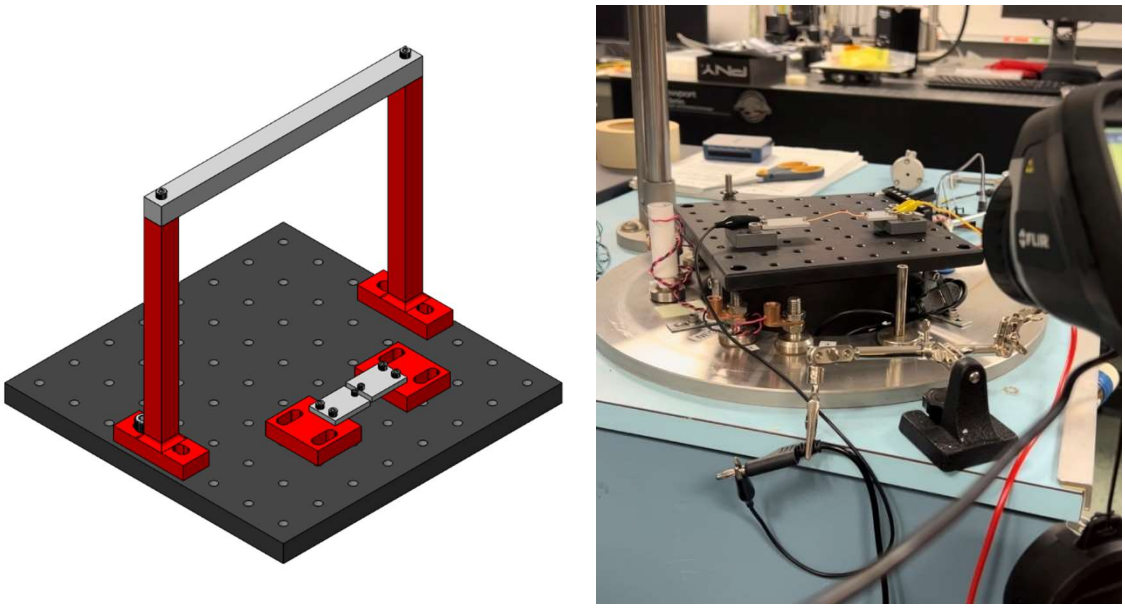

Figure 4.14 – Test Stand 3D CAD Model and Manufactured Stand During Testing.

The RIGOL DP832 programmable linear DC power supply unit was used to provide power to the circuit. The unit has two output modes: constant voltage and constant current. These two modes work in conjunction with one another to provide a constant power value to the circuit. The

maximum voltage value allowed is 30 V, and the maximum current value allowed is 3 A. These two values are easily adjustable and can be set where necessary given the testing scenario.

Figure 4.15 – RIGOL DP832 Power Supply Unit.

Using alligator clips, the RIGOL DP832 positive terminal for Channel 1 is connected to one side of the wire mount and the negative terminal is connected to the other side. A Nichrome wire is horizontally mounted between two screws on either side of the wire mount. The wire mount is adjustable to accommodate varying wire lengths. The thermal camera is placed in the same vertical plane as the wire and pushed in as close as it can get to the wire. Data is transmitted to the computer in real time and can be recorded for future analysis. After everything is set up, we are left with the following experimental set up.

Figure 4.16 – Experimental Setup.

The problem with thermal imagers is their inability to detect temperatures through glass without a viewport. Because of this fault, I was unable to conduct experiments in the vacuum chamber at this time. The window for the FLIR ResearchIR software during the tests in air resembled Figure 4.17 below. Included in Figure 4.18 is an image of what the wire looks like during testing at its equilibrium temperature.

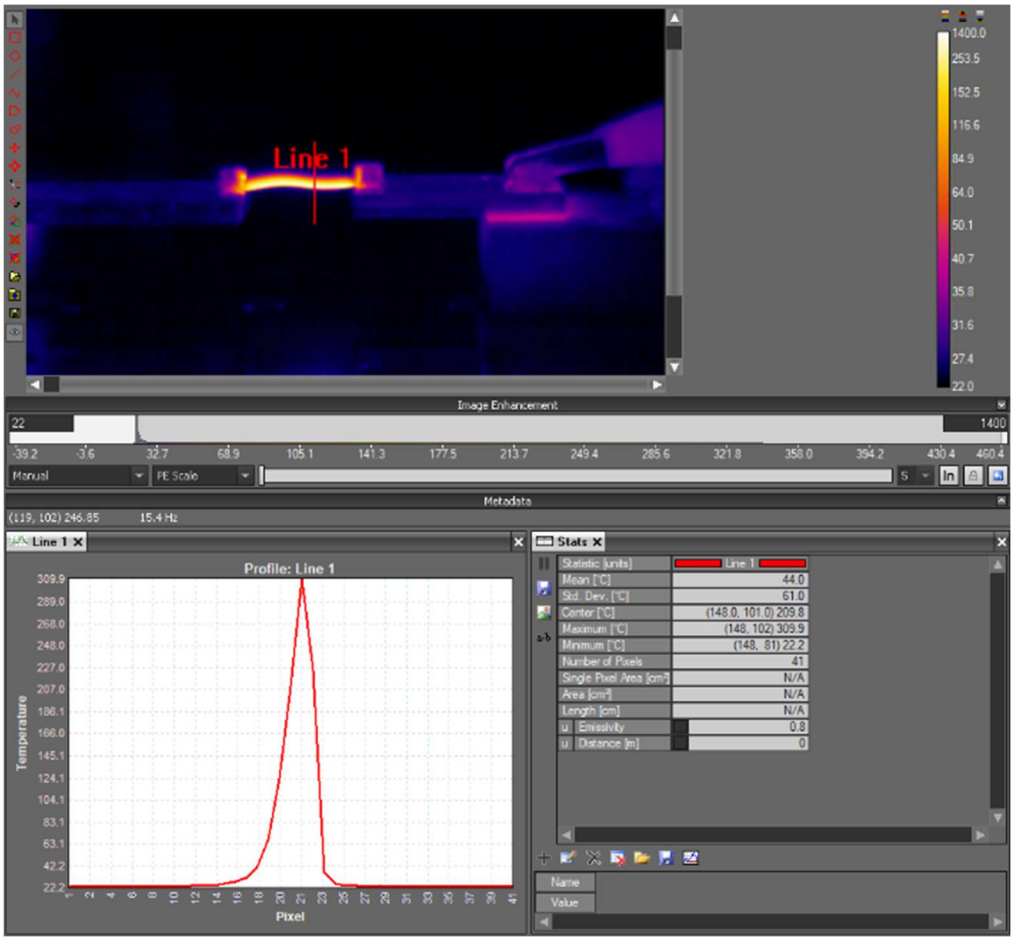

Figure 4.17 – FLIR ResearchIR Window During Experimentation.

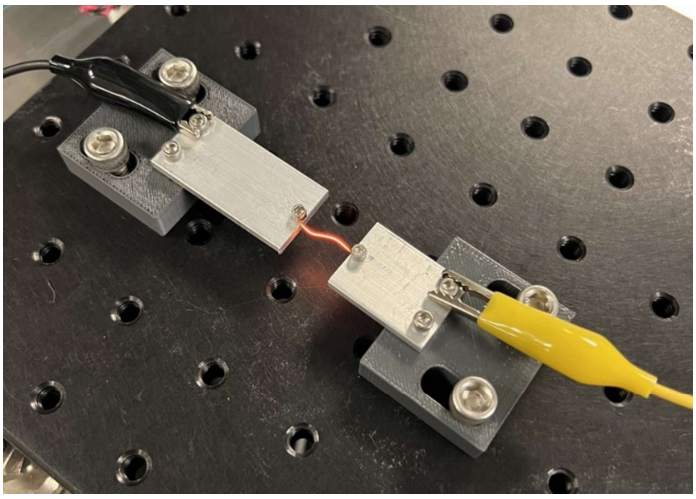

Figure 4.18 – Heated Wire During Experimentation.

5. RESULTS AND DISCUSSION

5.1 Analytical Results

As previously noted, due to the constant power in terms of Watts/inch, changing the length of the wire had no effect on the heating curve for wires of the same power ratio and gauge. Analytical data was recorded for both 40 Ga and 30 Ga wires for 0.5, 1, 1.5, 2, and 6 W/in, in both air and vacuum environments.

Analytical Values for Max Temp and Failure Time

Wire Gauge	Watts/inch	Environment	Max Temperature (°C)	Time to Failure (s)
40Ga	0.5	Air	1039.65	N/A
40Ga	0.5	Vacuum	1400.00	1.3062
40Ga	1	Air	1288.93	N/A
40Ga	1	Vacuum	1400.00	0.6531
40Ga	1.5	Air	1400.00	0.6000
40Ga	1.5	Vacuum	1400.00	0.4354
40Ga	2	Air	1400.00	0.4000
40Ga	2	Vacuum	1400.00	0.3265
40Ga	6	Air	1400.00	0.1300
40Ga	6	Vacuum	1400.00	0.1088
30Ga	0.5	Air	658.02	N/A
30Ga	0.5	Vacuum	1400.00	13.2717
30Ga	1	Air	881.93	N/A
30Ga	1	Vacuum	1400.00	6.6358
30Ga	1.5	Air	1018.86	N/A
30Ga	1.5	Vacuum	1400.00	4.4238
30Ga	2	Air	1118.57	N/A
30Ga	2	Vacuum	1400.00	3.3178
30Ga	6	Air	1400.00	1.4400
30Ga	6	Vacuum	1400.00	1.1059

Figure 5.1 – Analytical Calculations Results for Max Temperatures and Failure Times.

Due to the thicker diameter of the 30 Ga wire, it requires much more power per length to get it to heat up past the melting point threshold in the air environment. A maximum equilibrium temperature is reached due to the interacting heat transfer modes in the air environment and this value must exceed the melting point of the Nichrome wire for the wire to fail. In the vacuum environment, the melting point is always reached no matter what the gauge of the wire is, it just takes longer for the wires with thicker gauges.

5.2 SolidWorks Results

The same scenarios were run in SolidWorks, and the max temperatures and failure times were taken from the heating curves for the thermal sensor and tabulated.

SolidWorks Values for Max Temp and Failure Time

Wire Gauge	Watts/inch	Environment	Max Temperature (°C)	Time to Failure (s)	% Error SW
40Ga	0.5	Air	943.74	N/A	N/A
40Ga	0.5	Vacuum	1,400.00	1.3062	0%
40Ga	1	Air	1,225.10	N/A	N/A
40Ga	1	Vacuum	1,400.00	0.6531	0%
40Ga	1.5	Air	1,400.00	1.2000	100%
40Ga	1.5	Vacuum	1,400.00	0.4354	0%
40Ga	2	Air	1,400.00	0.5000	25%
40Ga	2	Vacuum	1,400.00	0.3265	0%
40Ga	6	Air	1,400.00	0.1500	15%
40Ga	6	Vacuum	1,400.00	0.1088	0%
30Ga	0.5	Air	548.62	N/A	N/A
30Ga	0.5	Vacuum	1,400.00	13.2717	0%
30Ga	1	Air	776.12	N/A	N/A
30Ga	1	Vacuum	1,400.00	6.6358	0%
30Ga	1.5	Air	922.48	N/A	N/A
30Ga	1.5	Vacuum	1,400.00	4.4238	0%
30Ga	2	Air	1,033.00	N/A	N/A
30Ga	2	Vacuum	1,400.00	3.3178	0%
30Ga	6	Air	1,400.00	2.0000	39%
30Ga	6	Vacuum	1,400.00	1.1059	0%

Figure 5.2 – SolidWorks Results for Max Temperatures and Failure Times.

In comparison to the analytical calculations, the results for the vacuum simulations were spot on. The air simulations ranged in error from 15%-100%, indicating there may be an error with the simulation setup that is making it take longer for the wires to reach melting temperature.

5.3 COMSOL Results

The same scenarios were run in COMSOL, and the max temperatures and failure times were taken from the heating curves for the 3D cut point and tabulated.

COMSOL Values for Max Temp and Failure Time

Wire Gauge	Watts/inch	Environment	Max Temperature (°C)	Time to Failure (s)	% Error COMSOL
40Ga	0.5	Air	794.45	N/A	N/A
40Ga	0.5	Vacuum	1400.00	1.3060	0.01%
40Ga	1	Air	1030.75	N/A	N/A
40Ga	1	Vacuum	1400.00	0.6530	0.01%
40Ga	1.5	Air	1186.01	N/A	N/A
40Ga	1.5	Vacuum	1400.00	0.4353	0.02%
40Ga	2	Air	1304.80	N/A	N/A
40Ga	2	Vacuum	1400.00	0.3265	0.01%
40Ga	6	Air	1400.00	0.13	0.00%
40Ga	6	Vacuum	1400.00	0.1088	0.02%
30Ga	0.5	Air	453.10	N/A	N/A
30Ga	0.5	Vacuum	1400.00	13.2717	0.00%
30Ga	1	Air	645.40	N/A	N/A
30Ga	1	Vacuum	1400.00	6.6355	0.00%
30Ga	1.5	Air	767.01	N/A	N/A
30Ga	1.5	Vacuum	1400.00	4.4238	0.00%
30Ga	2	Air	858.59	N/A	N/A
30Ga	2	Vacuum	1400.00	3.3178	0.00%
30Ga	6	Air	1269.50	N/A	N/A
30Ga	6	Vacuum	1400.00	1.1059	0.00%

Figure 5.3 – COMSOL Results for Max Temperatures and Failure Times.

Just like the SolidWorks vacuum simulations, the COMSOL vacuum simulations were very similar to the analytical calculations. The air simulations struggled to reach melting temperatures, however the one air simulation that did achieve failure matched up with the analytical calculation. This likely has something to do with how the air simulations were set up since the heat transfer modes that are removing energy from the wire are removing more than expected.

5.4 Experimental Results

For the physical experiments, only 40 Ga wire was tested due to time limitations and available materials. 0.5-inch-long wire was tested because it was the shortest length that was

easy to repeatedly tie around the screws after wire failures. This wire was tested at all the Watts/inch values used previously.

Experimental Values for Max Temp

Wire Gauge	Watts/inch	Environment	Max Temperature (°C)
40Ga	0.5	Air	75.40
40Ga	1	Air	124.70
40Ga	1.5	Air	164.20
40Ga	2	Air	195.40
40Ga	6	Air	340.10

**Failure Temp = ~390°C*

Figure 5.4 – Experimental Results for Max Temperatures.

According to the software, the maximum possible temperature that the wire could achieve before failure was around 390°C. I assume this is an error resulting from the output values needing to be scaled due to the detectable temperature range of the camera of 0°C to +650°C. This could potentially be fixed using a scaling equation by dividing the analytical heating curve by the experimental heating curve and then using the solution as a function that can be multiplied by the experimental data to get data that matches the analytical solutions. Ultimately the experimental data should be the most reliable since it is real world data, but these results are considerably off what is expected.

6. CONCLUSIONS

The results gathered in this report yield multiple conclusions that can be used for further investigation into this topic. The theoretical background behind the joule heating of Nichrome burn wires was examined and used to generate analytical results. This theory was also used to develop similar simulations that yielded similar results to the analytical results. Physical experiments were conducted to see the real-world effects of joule heating in person, and this helped me to better understand what it takes to create a properly working and well thought out experiment. Though the physical experiments yielded poor data, manufacturing and test setup skills were learned that can be carried into the future. Investigations into substitutions for the standard Nichrome burn wire mechanism are an important topic in the industry, so this research is important for our CubeSat program. The objectives I set for myself with this research were achieved and will make for a great starting point for further research in my master's studies.

7. FUTURE WORK

Since I plan to pursue my master's studies and focus on this same topic, there are several goals I have for the future of this research. Some of the goals I have for this research are:

- Properly configure the thermal imager to gather accurate data, ideally beyond 650°C (buy a filter or maybe get a new camera).
- Investigate the effects that tensile forces acting on the wire have on the time to failure.
- Run similar studies on all wire gauges ranging from 30 Ga to 40 Ga, not just the extremes.
- Look into constant voltage/current methods as opposed to just constant power.
- Investigate alternatives to burn wire mechanisms such as shape-memory alloy actuators (this is what the Aerospace Corporation uses because with Nichrome burn wire mechanisms you can never test what you fly because they are prone to failure during testing [13]).
- Develop more proficient skills in using SolidWorks and COMSOL simulations and learn to use LabView and MATLAB in collaboration with simulations/physical experiments so that processes can be more automated.

8. REFERENCES

[1] "CubeSats in a nutshell." *Government of Canada*. 6 May 2022. https://www.asc-csa.gc.ca/eng/satellites/cubesat/what-is-a-cubesat.asp.

[2] "History of the CubeSat." *SPACE DAILY*. 23 August 2016. https://www.spacedaily.com/reports/History_of_the_CubeSat_999.html.

[3] Novak, Alexandra, Schuett, Ashley, and Parker, Alison. "The Rise of CubeSats: Opportunities and Challenges." *Wilson Center*. 7 February 2022. https://www.wilsoncenter.org/blog-post/rise-cubesats-opportunities-and-challenges.

[4] Wiens, Kyra. "CubeSat Release Mechanism for Solar Panel and Tether Deployment Invented." *SatMagazine*. October 2014. http://satmagazine.com/story.php?number=1998655929

[5] "CubeSat 101: Basic Concepts and Processes for First-Time CubeSat Developers." *NASA*. October 2017. https://www.nasa.gov/sites/default/files/atoms/files/nasa_csli_cubesat_101_508.pdf

[6] "Thermal Analysis with SOLIDWORKS Simulation textbook." *Dassault Systems*. https://www.solidworks.com/partner-product/thermal-analysis-solidworks-simulation-textbook

[7] "Heat Transfer Module: Analyze Thermal Effects with Advanced Simulation Software." *COMSOL*. https://www.comsol.com/heat-transfer-module

[8] "The Joule Heating Interface." *COMSOL*. https://doc.comsol.com/5.5/doc/com.comsol.help.comsol/comsol_ref_heattransfer.21.15.html

[9] "Technical Data: FLIR E60 (incl. Wi-Fi)." *FLIR*. https://www.globaltestsupply.com/pdfs/cache/www.globaltestsupply.com/flir_systems/thermal_imager/e60/manual/flir_systems_e60_thermal_imager_manual.pdf

[10] "RIGOL User's Guide: DP800 Series Programmable Linear DC Power Supply." *RIGOL.* June 2016. https://www.globaltestsupply.com/pdfs/cache/www.globaltestsupply.com/dp832/manual/dp832-manual.pdf

[11] DeepBlueHarp. "Calculating Wire Temperature is Not Complicated (Nichrome example)." *Youtube*. 2 April 2018. https://www.youtube.com/watch?v=QNS0LrlRHbs

[12] "ResearchIR 4: User's Guide." *FLIR*. 10 February 2015. https://assets.tequipment.net/assets/1/26/FLIR_ResearchIR_User_Manual.pdf

[13] Welle, Richard, Fuller, Jerry, and Hardy, Brian. "Shape-Memory Alloy Actuators for Small Satellites." *Small Satellite* Conference. 5 August 2017. https://digitalcommons.usu.edu/smallsat/2017/Alternates/7/